

Design of the E-Patch Dual-Band Microstrip Antenna with Low Reflections for WLAN Application

Fubara Edmund Alfred-Abam*

Department of Electrical & Electronics Engineering, Bells University of Technology, Nigeria

Email: abamfubara@yahoo.com

Pam Paul Gyang

Department of Electrical & Electronics Engineering, University of Lagos, Nigeria

Email: gyangpaulpam@gmail.com

Received: 15 September, 2022; Revised: 31 October, 2022; Accepted: 25 November, 2022; Published: 08 February, 2023

Abstract: Antennas are either massive or miniaturized structures useful for the transmission and reception of signals associated with Electromagnetic (EM) radiation. Although Microstrip Patch Antennas (MSA) are advantageous they exhibit several drawbacks which may impair a faster communication throughput. They mostly display narrow impedance bandwidth amidst other grave issues. This study presents some approaches such as transmission line analysis and modeling for investigating the complexities associated with the MSA configurations given the shortcomings of narrow impedance bandwidth. In order to achieve the associated input impedance for the dual-band E-patch microstrip antenna. It also investigated the fabrication of the E-patch MSA which targeted the operating frequencies of 2.4 GHz and 5.8 GHz for possible range and speed. The fabricated prototype was tested using a high-frequency communication instrument known as the Vector Network Analyzer (VNA) to obtain the return loss and Voltage Standing Wave Ratio (VSWR). This method was done to quantify the reduction of reflections for enhanced Radio Frequency (RF) network output. This work helps to mitigate the challenges encountered when designing and developing microstrip patch antennas having a relatively small size in different configurations.

Index Terms: Dual Band, Input Impedance, Microstrip Patch Antenna, Radio Frequency, Return loss, Vector Network Analyzer, Voltage Standing Wave Ratio.

1. Introduction

Antennas are the interface between radio waves propagating through space by electric currents moving in metal conductors like transmission lines [1]. A microstrip antenna is a transmission line that consists of a conductor fabricated on a dielectric substrate with a ground plane. They can be easily miniaturized and integrated into a microwave, wireless communication, and several other systems, and are considered significant depending on their mode of configuration and operational applicability. The current trend in antenna design involves both computer simulation and experimental developments. The combination of both is advantageous as it improves creativity and productivity, capable of sustaining high performance over a large frequency spectrum. In light of modern technological applications, designing a minimal-weight, low-cost antenna capable of maintaining high performance focuses more on Microstrip Patch Antennas (MSA).

The microstrip patch antennas conventionally exhibit inherent narrow impedance bandwidth because of their inverse relationship between the relative permittivity of substrates. The intrinsic nature of the MSA also contributes to the impairment of signals, and these physical disadvantages are a result of low-power handling capacity, surface waves excitation, low gains and exhibit spurious feed radiation [2]. Furthermore, most WLAN experience overcrowding due to other relative signals operating on the same 2.4 GHz frequency. Although, there are different types of existing MSA enhancement techniques such as parasitic patches, Defected Ground Structure (DGS), shorting pins, Electromagnetic Band-Gap (EBG) and so on, each one of them has its benefits and negative marks [3]. However, the issue of impedance matching has also received less attention in many existing studies on microstrip patch antenna general performance. In this study, an attempt is made to tackle the issues of impedance matching in order to enhance the antenna's general

performance. The concept focuses on slot variations and iterative parametric changes, which affect the antenna performance in terms of the impedance bandwidth, return loss, VSWR and polarization, and other related parameters.

Therefore, there is a need to intensify research to examine the stated problems to design a more compact antenna capable of high-performance communication with less noise interference. This is the research direction being followed in this work, and it focuses on the development of an E-patch MSA as a means to address the shortcomings and challenges of signal impairment.

2. Literature Review

a) Transmission Line Analysis

Transmission line in this context can be represented as an infinite series of two-port elementary components R, L, C, and G which are labeled as the four primary line constants [4,5]. A perfect transmission line will convey an electrical signal from source to load regardless of the rate of change in voltage. Figure 1 shows the equivalent circuit of a short length transmission line, analyzed as a small differential point, where $V(x,t)$, $I(x,t)$, R_x , L_x , and C_x are the input voltage, input current at the node, resistive component, inductive component, conductive component, and capacitive component with respect to the length of a small segment characterized by x .

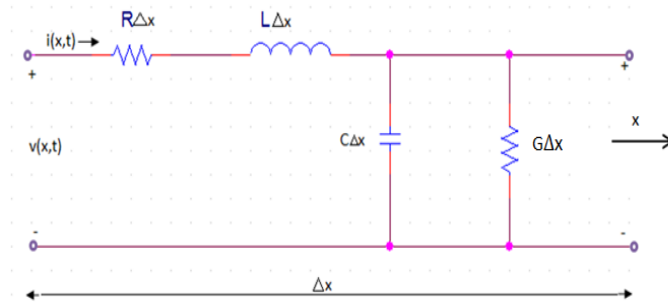


Fig. 1. Elementary component of a section of transmission line

By applying KVL to the circuit, the voltage across the inductor and resistor is considered and analyzed in series according to Eqs. (1) and (2):

$$V(x) - V(x + \Delta x) = \frac{\partial I(x)}{\partial t} L \Delta x + I(x) R \Delta x \quad (1)$$

$$-\frac{\partial V}{\partial x} \Delta x = \frac{\partial I}{\partial t} L \Delta x + I R \Delta x \quad (2)$$

The rate of change of voltage with respect to x at a particular time is a function of the rate of change of current with time. Hence, by applying KCL into the capacitive element shunt analysis is therefore considered as described by Eq. (3) and (4):

$$I(x) - I(x + \Delta x) = \frac{\partial V(x)}{\partial t} C \Delta x + V(x) G \Delta x \quad (3)$$

$$-\frac{\partial V}{\partial x} \Delta x = \frac{\partial V}{\partial t} C \Delta x + V G \Delta x \quad (4)$$

For time harmonics $\frac{\partial}{\partial t}$ is replaced by $j\omega$ hence as represented by Eqs. (5) and (6):

$$\frac{\partial V(x)}{\partial x} = -(R + j\omega L) I(x) \quad (5)$$

$$\frac{\partial I(x)}{\partial x} = -(G + j\omega C) V(x) \quad (6)$$

Second order differential equation on V & I with respect to x will result in the change as defined by Eqs. (7) and (8):

$$\frac{\partial^2 V}{\partial x^2} = -(R + j\omega L) \frac{\partial I}{\partial x} \quad (7)$$

$$\frac{\partial^2 I}{\partial x^2} = -(G + j\omega C) \frac{\partial V}{\partial x} \quad (8)$$

By substituting Eqs. (5) and (6) into Eqs. (7) and (8) results in getting Eqs. (9) and (10):

$$\frac{\partial^2 V}{\partial x^2} = (R + j\omega L)(G + j\omega C)V \quad (9)$$

$$\frac{\partial^2 I}{\partial x^2} = (G + j\omega C)(R + j\omega L)I \quad (10)$$

From this juncture analyzing the series and parallel elements of the transmission line equivalent circuit, Kirchoff's law permits adding impedance (Z) in series and admittance (Y) in the parallel configuration [6] according to Eqs. (11) and (12).

$$Z = R + j\omega L \quad (11)$$

$$Y = (G + j\omega C) \quad (12)$$

Because of this relationship, the transmission line can also be described in derived parameters, namely the propagation constant gamma " γ " [6] according to Eq. (13).

$$\gamma = \sqrt{ZY} = \sqrt{(R + j\omega L)(G + j\omega C)} \quad (13)$$

Eqs. (9) and (10) are similar to the electromagnetic propagation constant as defined by Eq. (14):

$$\frac{\partial^2 V}{\partial x^2} = \gamma^2 V \quad \text{or} \quad \frac{\partial^2 I}{\partial x^2} = \gamma^2 I \quad (14)$$

Where γ is dimensionless and a complex quantity having a real part named Alpha (α) attenuation constant, while Beta (β) is a function of Omega (ω) phase constant according to Eq. (15)

$$\gamma = \alpha + j\beta \quad (15)$$

Hence, the general solution can then be obtained via solving the homogeneous second order linear equation and if roots are complex then the Eqs. is represented by (16) and (17) respectively.

$$V = A_1 e^{-(\alpha + j\beta)x} + B_2 e^{(\alpha + j\beta)x} \quad (16)$$

$$I = C_1 e^{-(\alpha + j\beta)x} + D_2 e^{(\alpha + j\beta)x} \quad (17)$$

Therefore by differentiating Eq. (18) and (19):

$$\frac{\partial V}{\partial x} = \gamma(-A_1 e^{-\gamma x} + B_2 e^{\gamma x}) \quad (18)$$

$$\frac{\partial I}{\partial x} = \gamma(-C_1 e^{-\gamma x} + D_2 e^{\gamma x}) \quad (19)$$

Substituting Eqs. (18) and (19) into Eqs. (20) and (21):

$$-(R + j\omega L)I = \gamma(-A_1e^{-\gamma x} + B_2e^{\gamma x}) \quad (20)$$

$$-(G + j\omega C)V = \gamma(-C_1e^{-\gamma x} + D_2e^{\gamma x}) \quad (21)$$

From this point the relationship between the V & I are integrated in order attain the characteristic impedance (Z_0) according to Eq. (22):

$$I = -\frac{\gamma}{(R + j\omega L)}(-V_1e^{-\gamma x} + V_2e^{\gamma x}) \quad (22)$$

Replacing propagation constant by series impedance and shunt admittance as define by Eq. (23)

$$I = -\sqrt{\frac{(R + j\omega L)(G + j\omega C)}{(R + j\omega L)}}(-V_1e^{-\gamma x} + V_2e^{\gamma x}) \quad (23)$$

$$I = \sqrt{\frac{(G + j\omega C)}{(R + j\omega L)}}(-V_1e^{-\gamma x} + V_2e^{\gamma x}) \quad (24)$$

Eq. (24) can be translated to the transmission line and load equation considering the driving function as described by Eq. (25)

$$I = \frac{1}{Z_0}(-V_1e^{-\gamma x} + V_2e^{\gamma x}) \quad (25)$$

Hence, the characteristic impedance is given by Eq. (26):

$$Z_0 = \sqrt{\frac{(R + j\omega L)}{(G + j\omega C)}} \quad (26)$$

where R, G, L and C represents the resistance, conductance, inductance and capacitance of the transmission line. In place of calculating for the characteristics impedance, are fixed values 50 Ω or 75 Ω . These values are standard characteristics impedance of a short transmission line useful for antenna connection RF matching purposes [7]. At this juncture the reflection coefficient (Γ) is given by Eq. (27) [8]:

$$\Gamma = \frac{Z_{antenna} - Z_0}{Z_{antenna} + Z_0} \quad (27)$$

Where $Z_{antenna}$ and Z_0 , in this case, represent the load impedance and the characteristics impedance. However, in practice, Γ is usually expressed in dB [9]. Thus, by considering the voltage, the expression Γ in dB is given by Eq. (28):

$$\Gamma(dB) = -20 \log_{10} \Gamma \quad (28)$$

b) Related Review

Several related studies have been presented on the MSA aspects. For instance, a study has been presented on dual-band U-slot microstrip patch antenna for WLAN applications [10]. The authors presented a patch antenna design to address the issue of spurious feed radiation and interference. the aperture-coupled method was adapted in this study and the antenna was simulated under a frequency level of 3 GHz to 10 GHz, the antenna exhibited a dual-band mode, which occurs at 3.6 GHz and 5.2GHz. The return loss and VSWR results were satisfactory. In another study, the performance of a microstrip antenna was discussed, which was integrated with an Electromagnetic Band-Gap (EBG) substrate [11]. The paper emphasized the use of EBG substrate for surface wave reduction, to achieve an improved patch antenna performance. The antenna structure was made from the Flame Retardant (FR-4) substrate and operated at the 2.486 GHz wireless band. The outcome of this work reveals an improved return loss and gain.

A study has also been reported with a focus on proximity-coupled rectangular microstrip antenna with X-slot for wireless applications [12]. This research work expounded facts on spurious radiation elimination to achieve an improved bandwidth. The authors presented an antenna that operates at 2.45 GHz, proximity-coupled with a microstrip feed line method. A single-band mode was achieved, and the antenna can receive or transmit the signals at only that point of frequency.

Furthermore, an improved design of compact microstrip patch antenna for future 5G applications was presented [13]. This study was aimed at designing a miniaturized antenna to address the issue of large MSA sizes and low gain.

Lastly, a study was also discussed on the design and development of a symmetrical E-shaped to address the issue of interference [14]. The antenna was designed to have multiple slots-loading effects all around the patch peripheral which resulted in exhibiting five frequency bands ranging from 6.166 GHz to 10.500 GHz. This work revealed a significant reduction of the MSA, given the multiple resonance effect and having a miniaturized state.

Most of the reviewed patch antennas exhibit good features that can be applied to other applications, with just a few of them in the Wi-Fi application range. Some of the reflected magnitudes were not optimum at their resonant frequencies. Also, most of the papers focused on achieving either a single or multiple-band mode with minimal concerns about the general antenna size. The stack-up technique, i.e. the aperture-coupled, proximity-coupled and EBG structure method was identified in some of the reviews [10-12]. Considering modern-day trends of devices being miniaturized. Although these methods are good for eliminating spurious radiation, impedance matching becomes difficult because of the complexity of stacking [15].

3. Methodology

a) Conceptual Framework

This aspect of the work presents the design context. In Figure 2, several techniques are conceptually integrated and applied to attain better MSA performance. These include the following methods: impedance matching, parametric changes feeding technique and reactive loading. The idea of this research work is such that introduces MSA synthesis as one of the ways to bridge the identified gaps. This is done using the method of iteration and by implementing this process, the antenna behavior is ascertained in terms of structural modification. Numerous sub-layers are associated with these methods such as slot-loading and perturbation effects.

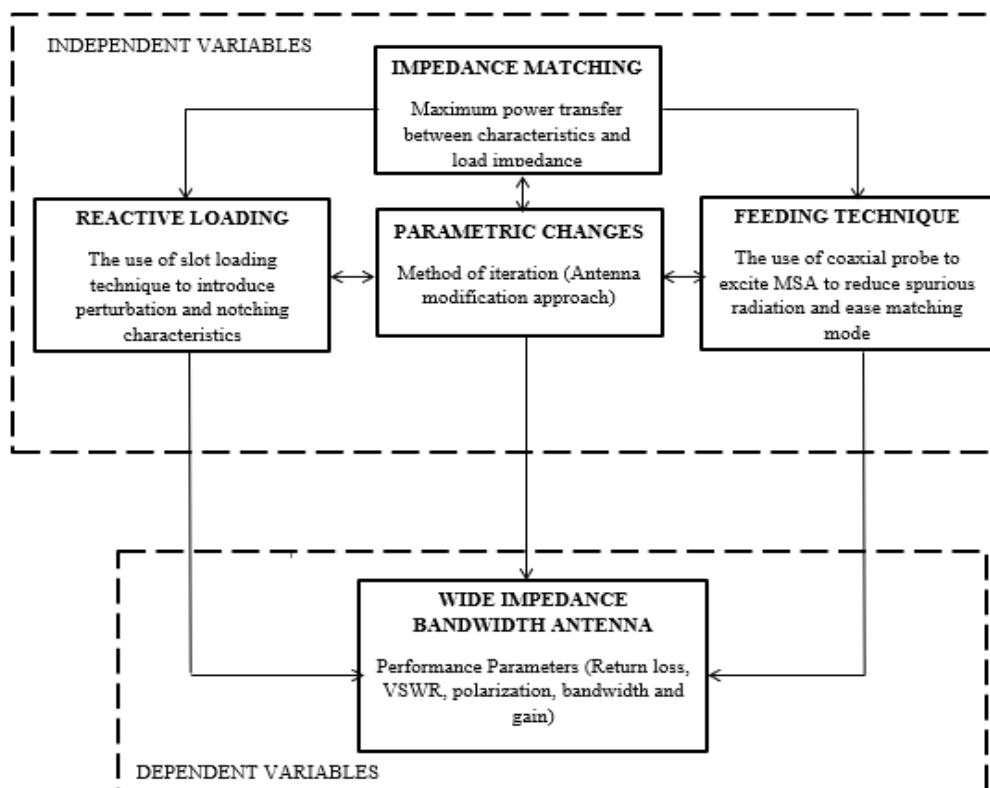


Fig. 2. Conceptual framework of the MSA

The conceptualization of the antenna involves the adaption of empirical formulas in conjunction with the Transmission Line Model (TLM) method of analysis. The antenna is further synthesized utilizing the ADS Full-Wave Simulation (FWS) software in line with the Finite Element Method (FEM) and Method of Moment (MOM). Figure 3 shows the block diagram of the design phases of the MSA. The design phases are categorized into five different subdivisions: design method, design challenges, design process, design parameters and design performance.

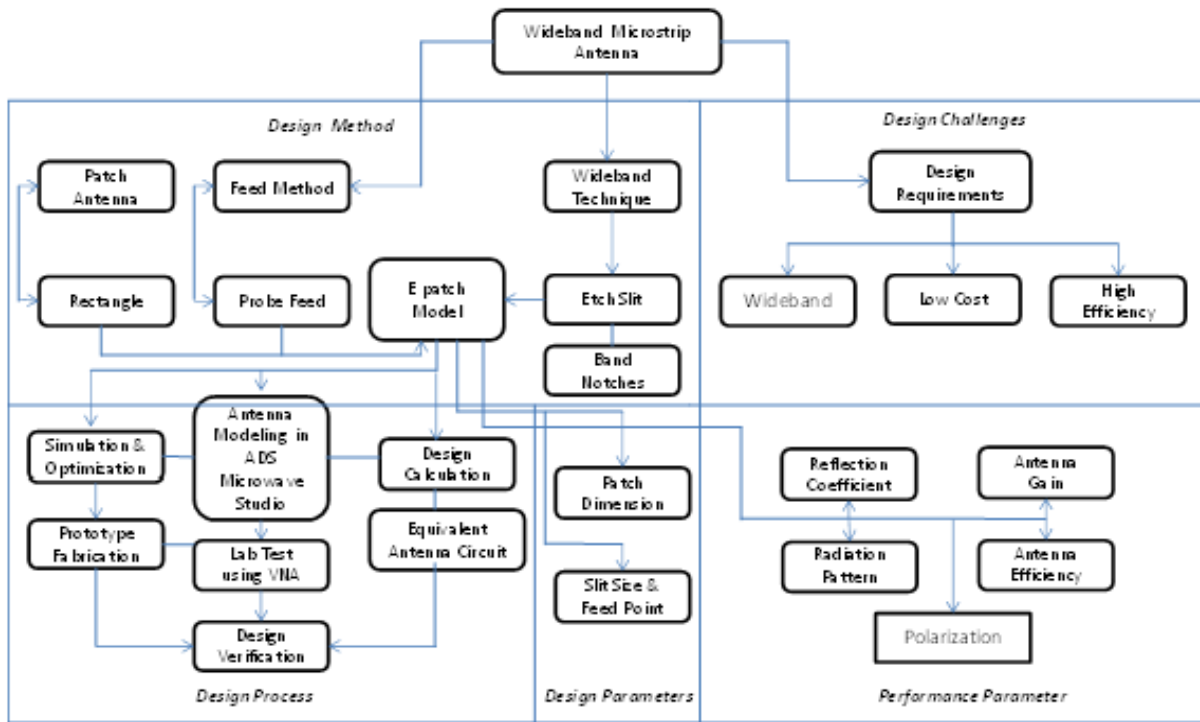


Fig. 3. Block diagram of design phases of the antenna.

b) Transmission Line Model Analysis

The Transmission Line Model (TLM) offers a good physical insight into driving the design to realize an arbitrary state. The TLM represents the MSA by two slots of the width and height separated by the length of the transmission line [16]. The heterogeneous nature of the two dielectrics (air and substrate) is a result of the E-field line having some part in the substrate and some in the air. As a result, the transmission line is unable to support a pure Transverse Electromagnetic (TEM) mode because the phase velocity is different in the two dielectrics. An alternative dominant mode of propagation was employed in this work; this is also known as the hybrid (Quasi-TEM). Since both fields travel in substrate and air, the need arises to calculate the effective dielectric constant (ϵ_{eff}) by also considering the air as a factor. Fig 4 shows the equivalence admittance circuit. The total admittance of slot 1 is obtained from transferring the admittance of slot 2 from the output terminal to the input terminal, by means of the admittance transformation equation for transmission lines [17] as described by Eq. (29).

$$Y_{in} = \left[Y_0 \frac{Y_0 + jY_s \tan(\beta L_1)}{Y_s + jY_0 \tan(\beta L_1)} + \frac{Y_0 + jY_s \tan(\beta L_2)}{Y_s + jY_0 \tan(\beta L_2)} \right] \quad (29)$$

where, Y_{in} , Y_0 , Y_s and β represent the input admittance, characteristics admittance, edge admittance and the phase constant. Hence, the input impedance of the transmission line is represented Eq. (30):

$$Z_{in} = \frac{1}{Y_{in}} \quad (30)$$

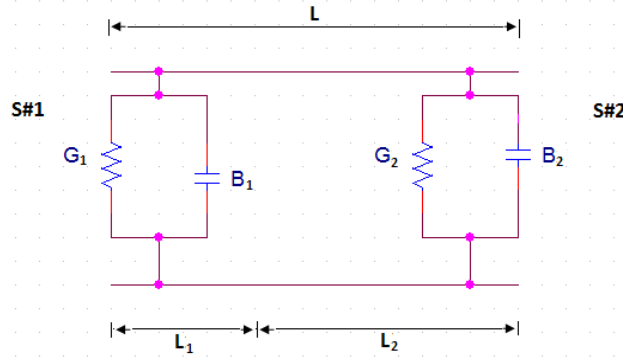


Fig. 4. Equivalent admittance circuit

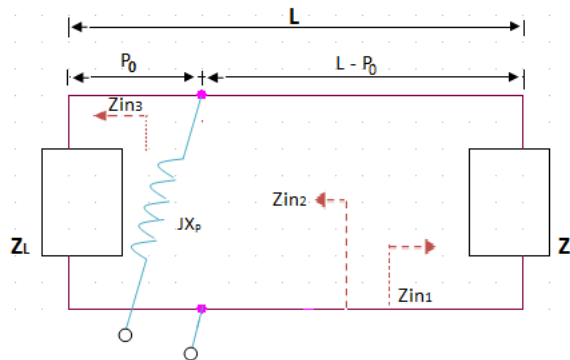


Fig. 5. Equivalent impedance circuit of the TLM

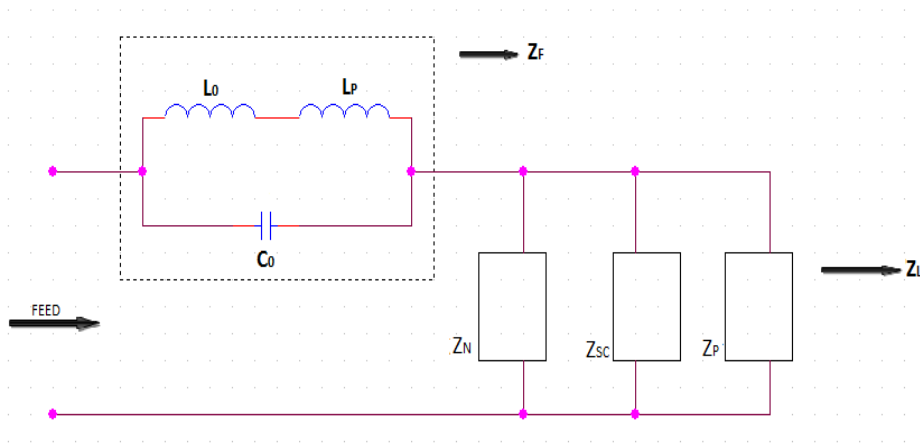


Fig. 6. The total equivalent input impedance of feed and slot loaded

The use of the Transmission Line Model (TLM) explores a thin substrate material having a low dielectric constant because it aids in suppressing the presence of greater surface waves. This yields a larger bandwidth, higher gain, and minimized cross-polarization towards achieving better antenna efficiency. The load impedance is enhanced by carrying out etching on the patch surface giving rise to perturbation, and notches. Figure 5 shows the equivalent circuit terminated with load. Figure 6 shows the total equivalent input impedance of the feed and the slot-loaded, where X_p , Z_F , Z_N , Z_{SC} , Z_P , L_0 , C_0 and L_p represent is the probe reactance, probe feed impedance, Notch Impedance, complementary slot impedance, patch Impedance, the static inductor, static capacitor and probe inductive reactance.

The total input impedance is represented by Eq. (31):

$$Z_{in_{total}} = JX_p + \left[\frac{Z_{in_1} \times Z_{in_2}}{Z_{in_1} + Z_{in_2}} \right] \quad (31)$$

c) Antenna Design Procedure

A suitable substrate material that satisfies the condition for WLAN application has been selected. The FR-4 epoxy is chosen, with the following specifications: having a dielectric constant of $\epsilon_r = 4.4$, material height, $h = 1.5\text{mm}$ and the intended operating frequencies f_o are 2.4 and 5.8 GHz. Also, the patch is fed by a $50\ \Omega$ coaxial probe. In order to design a dual-band antenna, both operating frequencies are targeted by creating two resonant modes on the patch. The frequency range hence has a low f_L and high f_H value, then the center frequency f_c is achieved [16] as described by Eq. (32).

$$f_c = \frac{f_L + f_H}{2} \quad (32)$$

The patch antenna coaxial probe technique can be adjusted to locate the perfect feed point. The desired input impedance is usually represented by Z and d is the position of the feed from the antenna [18]. The value of Z is described by Eq. (33):

$$Z = \frac{d}{2\sqrt{\epsilon_{eff}}} \quad (33)$$

The return loss and VSWR are important parameters that can be used to determine the reflection coefficient of an antenna. The return loss to VSWR basic conversion equation is used to maintain consistency in measurements [19] and is described Eq. (34).

$$VSWR = \frac{10^{\left(\frac{RL(dB)}{20}\right)_{+1}}}{10^{\left(\frac{RL(dB)}{20}\right)_{-1}}} \quad (34)$$

At this juncture, the arbitrary dimension of the rectangular patch is obtained by applying the TLM empirical technique. The E_{reff} is accounted for to enable a homogeneous propagation mode between the substrate and the air [16]. Hence, to satisfy the condition ϵ_{reff} the ratio of the patch antenna width to height must be greater than one ($W/h > 1$), and the length to height ($L/h > 1$) is also considered since it affects the fringing effect. Where, W , L and h represents the MSA width, length and antenna height.

The slot cut distribution method is employed where S_1 and L_1 represent the slot width and length. In order to achieve a symmetrical slot cut, the arbitrary W_{sp} is employed to characterize the summation of the perturbed patch width and W_s is used to represent the total slots according to Eqs. (35) and (36) in the design process. Such a characterization was adopted from the E-patch antenna geometry Figure 7.

$$W_{sp} = W_1 + W_2 + W_3 \quad (35)$$

$$W_s = S_1 + S_2 \quad (36)$$

However, for the patch design to be realistic, the conditions in Eqs. (37) and (38) are employed.

$$\text{if } L_2 > 0 \text{ then } L - L_1 > L_2 \quad (37)$$

$$\text{if } W_{sp} > 0 \text{ then } W - W_s > W_{sp} \quad (38)$$

After identifying the above patch conditions, the adjustable ratio limit can be obtained from various ratios having to do with the patch length L , width W , slot length L_1 and the slot width W_s from the E-patch geometry. Table 1 shows several antenna ratios; these ratios form an important aspect of the design of the E-patch antenna and by combining them, they complement the design process by enabling flexibility. This provides a small range of ratios for the purpose of antenna synthesis.

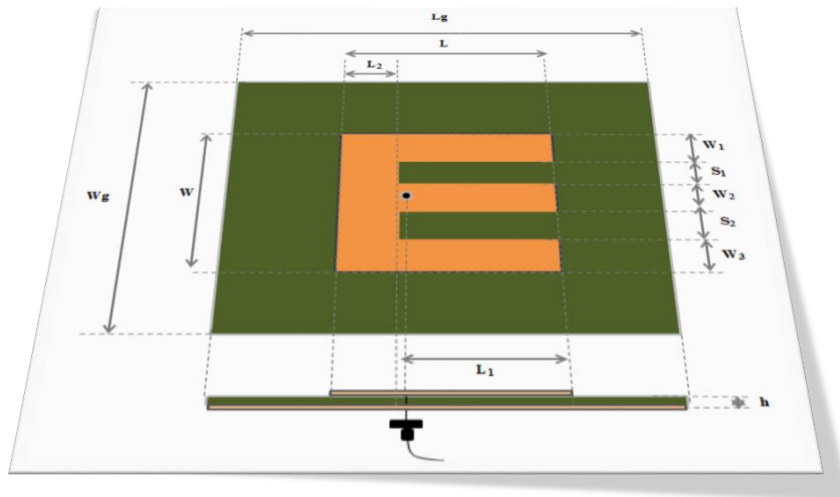


Fig. 7. E-patch antenna geometry

Table 1. The E-patch antenna ratios

Ratio	Values mm
W/L	1.31
L/W	0.76
L_1/L	0.73
W_s/W	0.4
L/L_1	1.35
W/W_s	2.5
W/L_1	1.77
L/W_s	1.90
L_1/W	0.56
W_s/L	0.52
L_1/W_s	1.40
W_s/L_1	0.71
L_2/L_1	0.35
W_{sp}/W_s	1.5
L_1/L_2	2.80

From this juncture, the design parameters were inputted and simulated using the Advanced Design System (ADS) full wave simulator to achieve an optimal impedance response. Figure 8 shows the related 3-dimensional simulated snapshots.

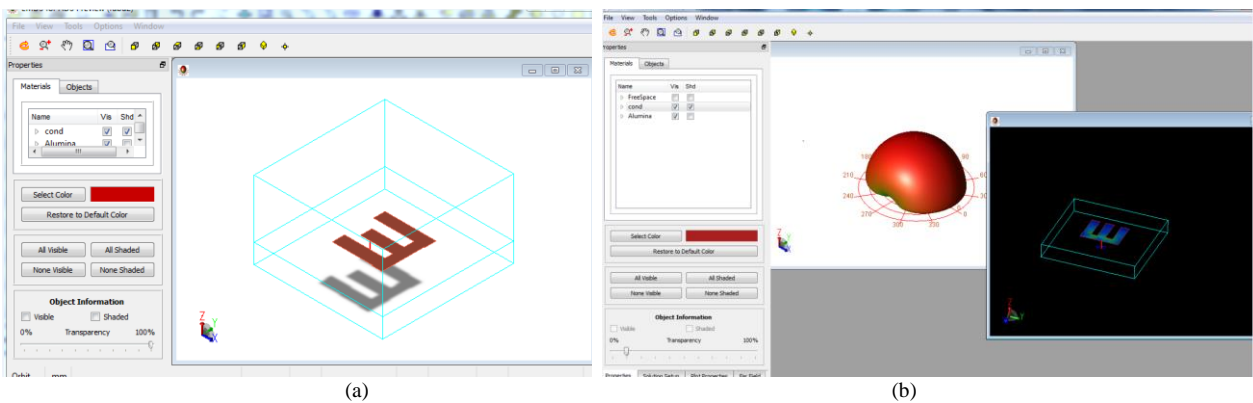
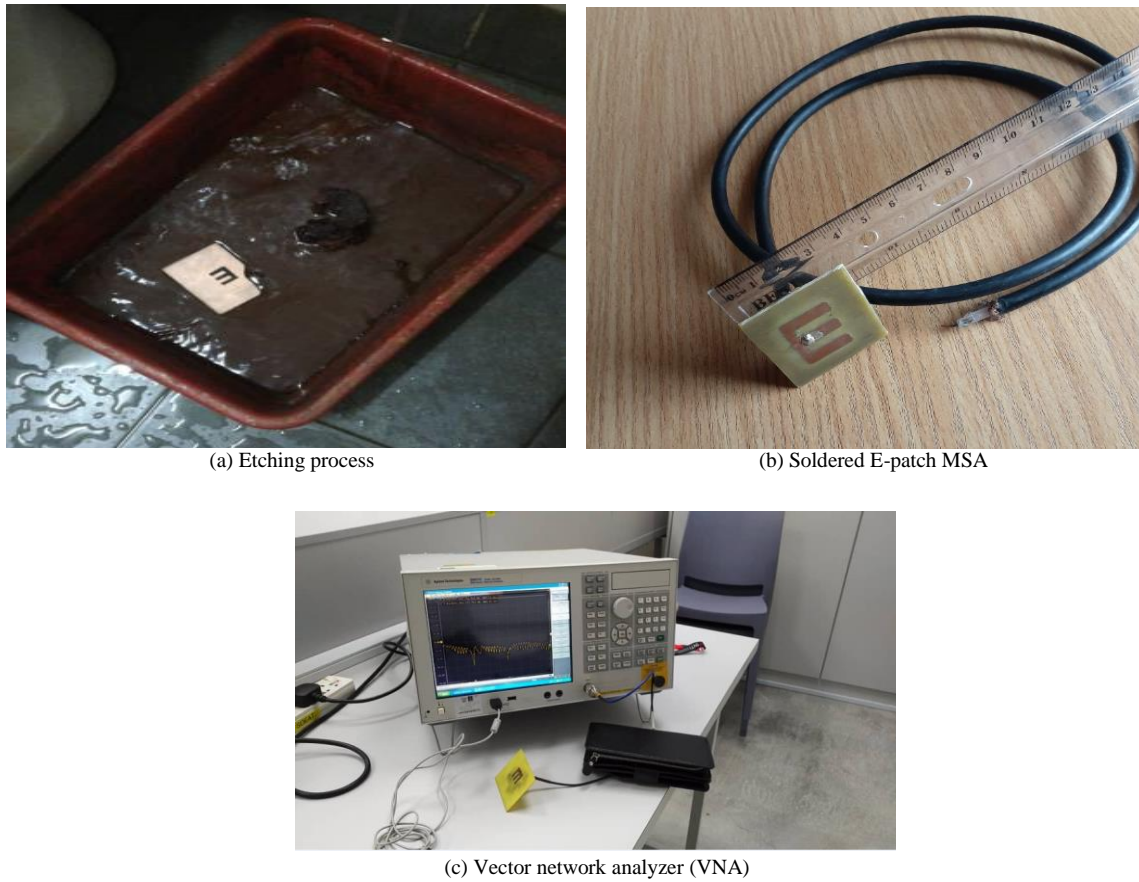


Fig. 8. (a)(b): Related 3-dimensional simulated snapshots

d) Fabrication and Testing

The fabrication process employed in this study is the IEEE Std. 145 Printed Circuit Board (PCB) processing method. The material used in this study is the FR-4 which involved the etching process and works by removing the unwanted copper region to retain the antenna's desired pattern. The copper region that is not protected by the etching resist is, therefore, etched out. The selected etchant chemical Ferric iron III chloride ($FeCl_3$) is employed for the fabrication process. The MSA was drilled with the coaxial cable soldered and tested using the Vector Network Analyzer (VNA).



(a) Etching process

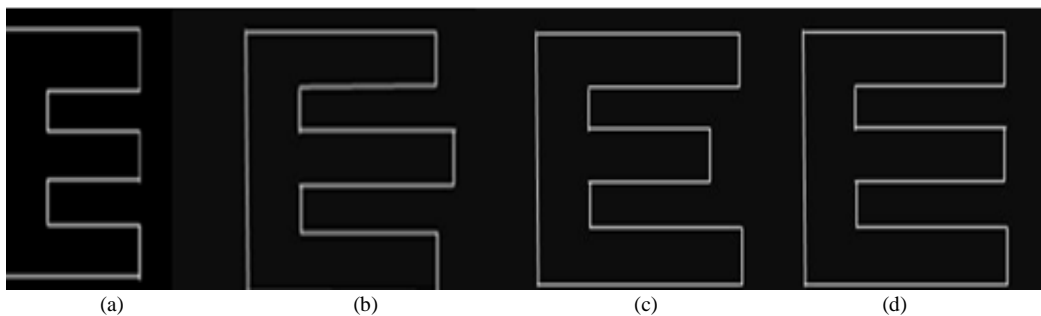
(b) Soldered E-patch MSA

(c) Vector network analyzer (VNA)

Fig. 9. (a)(b)(c): The E-patch microstrip antenna fabrication and testing process

4. Result and Discussion

This study revealed that the slot length L_1 was varied from 12.5 mm to 14.6 mm which was within the limit of the slot range. For a slot length lesser than 12.5 mm, there is little change in the surface current, and the second-order mode demonstrates a decrease in return loss. However, for a slot longer than 14 mm, the resonant mode shift arises. The process of redirecting the surface current to flow around a slot is a result of the parallel nature of the slot-loaded, which introduces a local inductive effect. Hence, a wider slot gives a higher inductive effect, which decreases the resonant frequency of the second-order mode. A slot width of 4.25 mm gives rise to an optimum dual-band mode and a slot width lesser or greater than this affects the frequency response.



(a)

(b)

(c)

(d)

Fig. 10. Several slot length and width variations

Figure 10 shows several structural modifications and the impact of their resonant frequency and return losses. Case (a) simulation was done for the first adaptive pass based on the arbitrary patch antenna parameters which had a non-optimal response. The simulated return loss result revealed the values of -32 dB at 2.4 GHz and -14 dB at 5.8 GHz, having a corresponding VSWR of 1.052 and 1.499. For case (b), the impact of the result showed a missed resonance which affected the value of the higher frequency by shifting the resonance to a much higher band. Case (c) on the other hand also exhibited a missed resonance which impacted the lower frequency with a shift in resonance to a higher band. Lastly, case (d) shows the optimal parametric result of the MSA and it was observed that the lower frequency band

resonates at 2.4 GHz with a return loss of -40 dB, while the upper-frequency band resonates at 5.8 GHz with a return loss of -35 dB, having a corresponding VSWR of 1.020 and 1.036.

The prototype test result plot showed a return loss of -36 dB at the lower frequency band 2.4 GHz. However, the upper-frequency band resonates at 5.8 GHz with a return loss of -31 dB. The VSWR value of 1.032 at 2.4 GHz and 1.052 at 5.8 GHz. In addition, the associated bandwidth for the lower frequency band is 0.12 GHz, while the higher frequency band is 0.26 GHz, respectively as seen in figure 11.

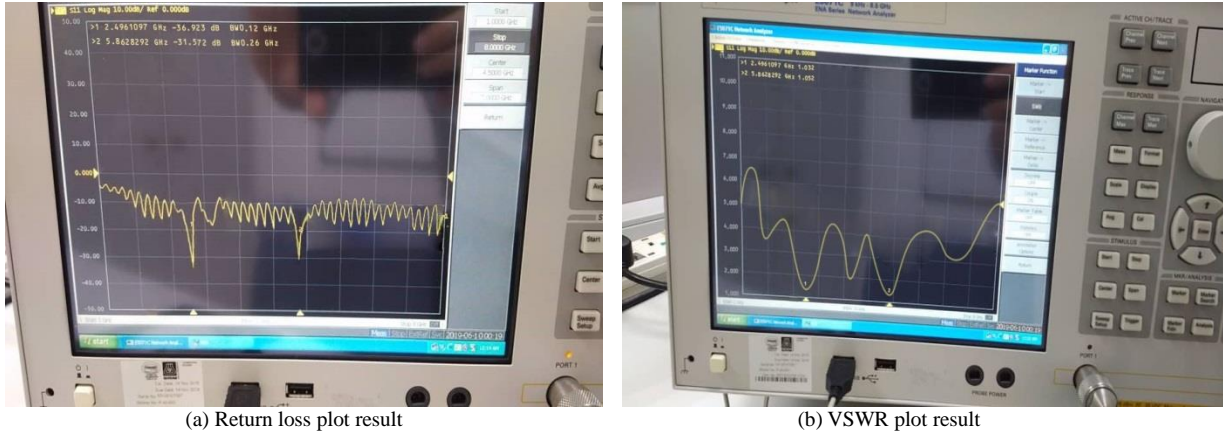


Fig. 11. (a) (b): VNA return loss and VSWR variation plot

To justify the above results, the return loss can be expressed in logarithmic form as given by Eq. (28). This implies the VSWR is related to the return loss and a considerable acceptable VSWR is less than 2, this signifies a good antenna match [20]. Hence, for a return loss of -10 dB a corresponding VSWR of 1.92 is associated. Figure 12 shows the comparison between the simulated and the fabricated test results reflection coefficient. The simulated and the fabricated results both correspond in terms of their frequency operation modes. However, they exhibit a slight discrepancy in terms of their reflection magnitudes, which is also acceptable. Having a very large magnitude difference may require re-design of the antenna, which is caused by either improper etching, leakage from the feed point, error in design equation, signal interference, or error in cable connection to test equipment.

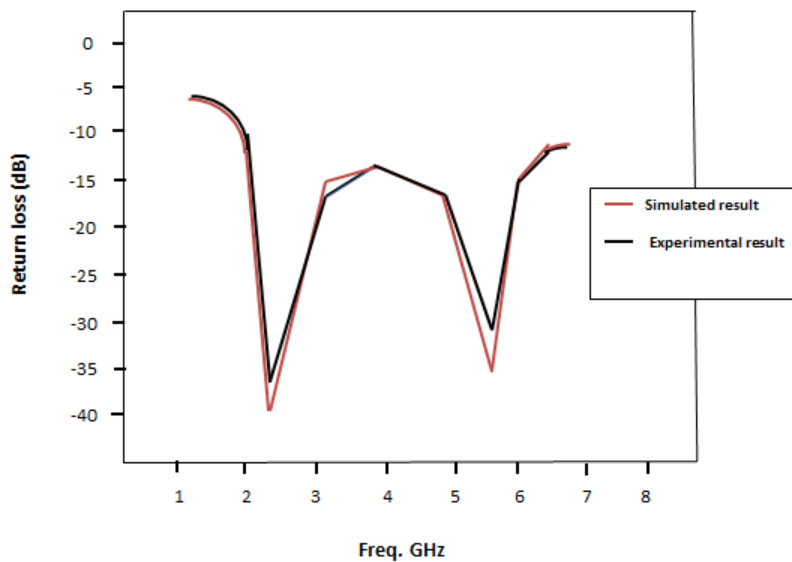


Fig. 12. Comparison between the simulated and fabricated return loss versus frequency

5. Conclusion

From the simulation and fabricated results, it is evident that the E-patch antenna provides a useful design that operates in a dual-band mode with resonating frequencies at 2.4 GHz and 5.8 GHz. The resultant S_{11} magnitudes are less than -20 dB, demonstrating a good percentage acceptance value of the signal reflected. Furthermore, realizing an antenna efficiency of 94% in the design, simulation and fabrication of the MSA is an indication that it is possible to develop, and manufacture efficient antennas on the micro-scale, hence, the microstrip design.

The significance of the E-patch antenna design is that it can contribute to a simultaneous dual-broadband radiation mode useful for high-performance wireless communication with less noise interference, having forward compatibility with recent Wireless Local Area Network (WLAN) technology. The antenna was designed to achieve a low reflection coefficient for the stated operating frequencies. These frequencies are allocated for possible range and speed, attributed to the S-band and C-band, respectively.

As technology generally approaches the 5th generation, antennas with a more complex design will be required to transmit data on such devices. The findings from this work will further aid designers and researchers in the field of antenna and propagation, providing substantial insight to advance the academic knowledge in communication engineering systems with particular emphasis on antenna design. As further work, the use of other antenna materials with high permittivity constant may be applied to investigate the suitability of other configuration.

References

- [1] Sharma, N and Vipul, S (2017). A Journal of Antenna Dipole to Fractal. *Journal of Engineering and Technology*. 6(2): 317-351.
- [2] Abdullahi, S.B.M. Shahanawaz, K. Ain M.F. and Zainal. A.A. (2019). Microstrip Patch Antenna: A Review and the Current State of the Art. *Journal of Advanced Research in Dynamical and Control Systems*. 11(7): 510-524.
- [3] Alok, K. Nancy, G. and Gautam, P.C. (2016). Gain and Bandwidth Enhancement Techniques in Microstrip Patch Antennas – A Review. *International Journal of Computer Application*. 148(7): 9-14.
- [4] Oke, M.O. (2017). An Analytical Method for Solving Wave Equations on Transmission Lines. *International Journal of Mathematics and Statistics Studies*. 5(3): 28-35.
- [5] Hasirci, Z. Cavdar, I.H. and Ozturk, M. (2018). RLGC(f) Modeling of a Busbar Distribution System via Measured S parameters at CENELEC and FCC bands. *Turkish Journal of Electrical Engineering and Computer Science*. 26(1): 489-500.
- [6] Unni, N.S. and Soumya, A.M. (2016). Transmission Line Characteristics. *IOSR Journal of Electronics and Communication Engineering*, 3(5): 67-77.
- [7] Carr, J.J. (2001). *Practical Antenna Handbook*, Fourth Edition. MacGraw-Hill. *United States of America*.
- [8] Roupheal, T. J. (2014). *Wireless Receiver Architectures and Design*. Antenna, RF, Synthesizer, Mixed Signal, and Digital Signal Processing. 1st Edition.
- [9] Ali, E. Khaled, E. and Hassan, B. (2012). Input Impedance, VSWR and Return Loss of a Conformal Microstrip Printed Antenna for TM₀₁ Mode using Two Different Substrates. *International Journal for Networks and Communications*. 2(2): 13-19.
- [10] Garima, K. A. and Khanna R. (2013). Dual and Triple Band U-Slot Microstrip Patch Antenna for WLAN Applications, *International Journal of Advanced Research in Computer and Communication Engineering*. 2(5): 2201-2204.
- [11] Tumsara, K.V. and Zade, P.L. (2016). Microstrip Antenna using EBG Substrate, *International Journal on Recent and Innovation Trends in Computing and Communication*. 7(8): 1573- 1577.
- [12] Sastry, I.V.S.R. and Sankar, K.J. (2014). Proximity Coupled Rectangular Microstrip Antenna with X-slot for WLAN Application. *Global Journal of Researches in Engineering: Electrical and Electronics Engineering*. 14(1):1-5.
- [13] Magaji, Y.R. Sulaiman, Y.Y. Babangida, M.M. Mustapha M.G. and Muhammad, S.A. (2018). Design of Microstrip Patch Antenna for Future 5G Applications. *International Journal of Advanced Academic Research Sciences, Technology and Engineering*. 4(7): 9-20.
- [14] Kaur, P. Singh, G. Jaspal, S. and Manjit, K. (2016). Design and Development of Symmetrical E-shaped Microstrip Patch Antenna for Multiband Wireless Applications. *International Journal of Signal Processing Image Processing and Pattern Recognition*. 9(10): 405-416.
- [15] Sharma, P. and Yadava, R.L. (2014). Comparative Analysis of Feeding Techniques for Microstrip Patch Antenna and Smart Antenna Applications in Mobile Communication. *IOSR Journal of Electronics and Communication Engineering (IOSR-JECE)*. 9(3): 25-30.
- [16] Balanis, A.C. (2005). *Antenna Theory, Analysis and Design*. Third Edition, New Jersey, Hoboken. John Wiley & Sons, Inc.
- [17] Sharma, S. Tripathi, C.C. and Rishi, R. (2017). Impedance Matching Techniques for Microstrip Patch Antennas. *Indian Journal of Science and Technology*, 10(28): 1-16.
- [18] Jasim, S.E. Jusoh, M.H. Mazwir, M.H. and Mahud, S.N.S. (2015). Finding the Best Feeding Point Location of Patch Antenna using HFSS. *ARPN Journal of Engineering and Applied Sciences*. 10(23): 17444-17449.
- [19] Base Station Transmits (2015). Method to Maintain Cable and Antenna Systems for Healthy Network Performance.[Online] Available :<https://anritsu.typepad.com/basestationtransmits/2015/06/methods-to-maintain-cable-and-antenna-systems-for-healthy-network-performance.html>.
- [20] Tong, T.C. (1973). Electromagnetic Scattering by a Thin Wire with Continuous Impedance Loading; Part II: Time Domain Analysis. *Electromagnetics Division Institute for Basic Standards National Bureau of Standards Boulder, Colorado 80302*.

Authors' Profiles



Dr. Fubara E. Alfred-Abam was born in Lagos State and hails from Okrika Rivers State Nigeria. He received his BEng. degree in Electrical and Electronics Engineering from the University of East London (UEL) in 2013, afterward pursued a MSc in Computer Systems Engineering from (UEL) in 2015. He obtained his Ph.D. in Electrical and Electronics Engineering from Bells University of Technology in 2021. He is vastly Knowledgeable in the areas of Electronics & Communication, Computer Networking, and Electrical Power systems. He currently works as a Lead Research and Development Engineer for EKEDC, Nigeria. His research interest includes Wireless Communication, Antenna & Wave Propagation, Transmission line and Power System

Distribution. He has published papers in International Journals and International Conferences.



Gyang Paul Pam was born in Plateau, Nigeria. He received a B.Sc. degree in Electrical and Electronics Engineering from the Federal University of Technology, Owerri, Nigeria in 2015, and is currently an MSc student at the University of Lagos, Akoka, Nigeria. He is a graduate research assistant to his supervisor who is a Postdoctoral Fellow at the Centre for Energy & Electric Power at the Tshwane University of Technology in 2022. Presently, Pam is a Research and Development/Simulation Engineer at Eko Electricity Distribution Company, Lagos. His current research interests lie in the areas of Lumped and Distributed Networks, Integration of Renewable Energy, Energy Harvesters, and Machine Learning Applications in Power System Resilience.

How to cite this paper: Fubara Edmund Alfred-Abam, Pam Paul Gyang, "Design of the E-Patch Dual-Band Microstrip Antenna with Low Reflections for WLAN Application", International Journal of Wireless and Microwave Technologies(IJWMT), Vol.13, No.1, pp. 14-26, 2023. DOI:10.5815/ijwmt.2023.01.02